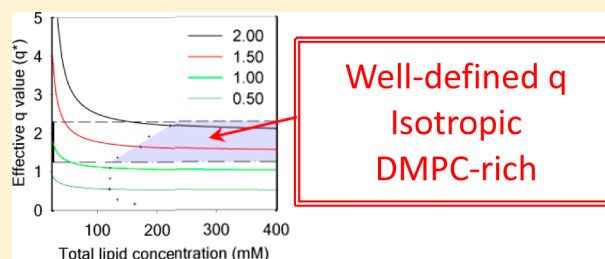


## Lipid Concentration and Molar Ratio Boundaries for the Use of Isotropic Bicelles

Maïwenn Beaugrand,<sup>†</sup> Alexandre A. Arnold,<sup>†</sup> Jérôme Hénin,<sup>‡</sup> Dror E. Warschawski,<sup>§</sup> Philip T. F. Williamson,<sup>||</sup> and Isabelle Marcotte<sup>\*,†</sup><sup>†</sup>Department of Chemistry, Université du Québec à Montréal and Centre Québécois sur les Matériaux Fonctionnels, P.O. Box 8888, Downtown Station, Montreal, Canada H3C 3P8<sup>‡</sup>Laboratoire de Biochimie Théorique, CNRS, Université Paris Diderot and Institut de Biologie Physico-Chimique, 13 rue Pierre et Marie-Curie, 75005 Paris, France<sup>§</sup>Laboratoire de Biologie Physico-Chimique des Protéines Membranaires, CNRS, Université Paris Diderot and Institut de Biologie Physico-Chimique, 13 rue Pierre et Marie-Curie, 75005 Paris, France<sup>||</sup>School of Biological Sciences, Highfield Campus, University of Southampton, Southampton, SO17 1BJ, United Kingdom

## S Supporting Information

**ABSTRACT:** Bicelles are model membranes generally made of long-chain dimyristoylphosphatidylcholine (DMPC) and short-chain dihexanoyl-PC (DHPC). They are extensively used in the study of membrane interactions and structure determination of membrane-associated peptides, since their composition and morphology mimic the widespread PC-rich natural eukaryotic membranes. At low DMPC/DHPC ( $q$ ) molar ratios, fast-tumbling bicelles are formed in which the DMPC bilayer is stabilized by DHPC molecules in the high-curvature rim region. Experimental constraints imposed by techniques such as circular dichroism, dynamic light scattering, or microscopy may require the use of bicelles at high dilutions. Studies have shown that such conditions induce the formation of small aggregates and alter the lipid-to-detergent ratio of the bicelle assemblies. The objectives of this work were to determine the exact composition of those DMPC/DHPC isotropic bicelles and study the lipid miscibility. This was done using <sup>31</sup>P nuclear magnetic resonance (NMR) and exploring a wide range of lipid concentrations (2–400 mM) and  $q$  ratios (0.15–2). Our data demonstrate how dilution modifies the actual DMPC/DHPC molar ratio in the bicelles. Care must be taken for samples with a total lipid concentration  $\leq 250$  mM and especially at  $q \sim 1.5$ –2, since moderate dilutions could lead to the formation of large and slow-tumbling lipid structures that could hinder the use of solution NMR methods, circular dichroism or dynamic light scattering studies. Our results, supported by infrared spectroscopy and molecular dynamics simulations, also show that phospholipids in bicelles are largely segregated only when  $q > 1$ . Boundaries are presented within which control of the bicelles'  $q$  ratio is possible. This work, thus, intends to guide the choice of  $q$  ratio and total phospholipid concentration when using isotropic bicelles.



## ■ INTRODUCTION

Bilayered micelles, or so-called bicelles, were introduced in the 1990s and quickly gained in popularity due to their similarity with biological membranes.<sup>1,2</sup> These membranes mimetics are most commonly composed of dimyristoylphosphatidylcholine (DMPC) which organize in a bilayer stabilized by short-chain dihexanoylphosphatidylcholines (DHPC) in high curvature regions<sup>3–8</sup> of discs or perforated vesicles.<sup>3–5,9–12</sup> Although the morphology of bicelles is debated, the planar region made of long-chain phospholipids constitutes a favorable environment to study molecular interactions as well as the structure of membrane peptides and proteins with different biophysical techniques such as nuclear magnetic resonance (NMR), X-ray crystallography, circular dichroism (CD), and Fourier transform infrared (FTIR) spectroscopy.<sup>3–5,10,13–18</sup> Most interestingly, for solid-state NMR applications, bicelles are known to

spontaneously orient in a magnetic field in excess of 1 T at high DMPC/DHPC molar ( $q$ ) ratios (above 2.3) and within well-defined total lipid concentrations (3–60% w/v) and temperatures (30–50 °C).<sup>2,5,11,12,19–23</sup> This orientation is due to the negative diamagnetic susceptibility anisotropy of the phospholipids which align with their long axis perpendicular to the magnetic field direction.

When the DMPC/DHPC  $q$  ratio falls below 2.3, bicelles rapidly reorient in solution,<sup>21,24,25</sup> enabling solution NMR experiments that are useful for the structural study of membrane-binding peptides such as met-enkephalin,<sup>26</sup> motilin,<sup>27</sup> antimicrobial peptides,<sup>28</sup> as well as the assessment of

Received: February 3, 2014

Revised: May 2, 2014

Published: May 5, 2014

membrane association of peptides and small molecules.<sup>26,29–31</sup> The use of low  $q$  ratio  $\leq 0.5$  allows improving the resolution of the NMR<sup>25,32</sup> and CD<sup>25,33–36</sup> spectra. These so-called isotropic bicelles are also employed in others studies such as dynamic light scattering (DLS),<sup>33,34</sup> FTIR spectroscopy,<sup>35</sup> fluorescence,<sup>36,37</sup> and electron paramagnetic resonance (EPR).<sup>38</sup> The morphology of isotropic bicelles is generally considered to be disc-shaped with DMPC molecules on the planar section segregated from the DHPC molecules in the rim, and a diameter which increases with  $q$  ratio.<sup>24,37</sup> The presence of transmembrane proteins in low  $q$  bicelles may however lead to a change in the size of the aggregates, as shown for micelles, and possibly to a reorganization of the lipids and detergents.<sup>39,40</sup>

Bicelles samples with a total lipid concentration lower than 150 mM are required with techniques using a laser light source to avoid light scattering effects when performing CD<sup>25,30,33–35</sup> or DLS,<sup>33,34</sup> but are also employed in other techniques such as NMR,<sup>29,33–35</sup> FTIR spectroscopy<sup>35</sup> and crystallography.<sup>15</sup> A thorough study of DMPC/DHPC bicelles in such conditions with  $q$  ratios from 0.5 to 5 was carried out by van Dam and co-workers<sup>41</sup> using cryo-transmission electron microscopy (TEM), DLS, and fluorescence spectroscopy. At  $q$  ratios below 1 and for strong dilutions, small aggregates were observed. This work also provided strong indications that the formed aggregates are more complex than the ideal bicelle model in which the DMPC and DHPC molecules are fully segregated. In addition, as was originally evidenced by Glover et al.,<sup>37</sup> the authors noted that dilution alters the actual composition of the aggregates. Indeed, the individual constituents of bicelles have specific critical micelle concentrations (CMCs) that can range from the nanomolar for the phospholipids, to the millimolar for the detergents. As a consequence, in samples prepared with concentrations in the millimolar range, a significant proportion of free surfactants in solution will be present in equilibrium with the phospholipid aggregate. The importance of this effect has recently been considered by the group of Sanders who has proposed alternative bicelles composed of surfactants with higher CMCs.<sup>42</sup> The widespread use of DMPC/DHPC bicelles prompted us to carry out a systematic study of the effect of dilution on this system.

The objective of this work is thus to study the effect of dilution on the exact composition of the widely utilized DMPC/DHPC bicelles and the miscibility of its constituents. Using <sup>31</sup>P NMR,  $q$  ratios ranging from 0.15 to 2 and concentrations from 2 to 400 mM are investigated. The work is carried without the use of paramagnetic shift reagents. The NMR results indicate changes in miscibility between short- and long-chain phospholipids and these are further supported by FTIR spectroscopy and molecular dynamics simulations. We thus provide data which will guide the choice of  $q$  ratio and total phospholipid concentration to enable the study of membranes and membrane-related processes using isotropic bicelles.

## MATERIALS AND METHODS

**Materials.** 1,2-Myristoyl-1-*sn*-glycero-3-phosphocholine (DMPC) and 1,2-hexanoyl-1-*sn*-glycero-3-phosphocholine (DHPC) were obtained from Avanti Polar Lipids (Alabaster, AL) and used without further purification. DHPC, which is highly hygroscopic, was freeze-dried prior to weighing. Deuterium oxide (D<sub>2</sub>O) was purchased from CDN Isotopes (Pointe-Claire, QC, Canada).

**Sample Preparation.** Bicelle samples with the highest concentration (400 mM) and at  $q$  ratios ranging between 0.25 and 2 were prepared by suspending the appropriate weight of DMPC and DHPC in a 100 mM KCl solution made with D<sub>2</sub>O. The sample was then submitted to 10 cycles of freeze (liquid N<sub>2</sub>)/thaw (60 °C) and vortex shaking, resulting in a uniform transparent nonviscous solution. Serial dilutions were then performed from 400 to 2 mM before NMR spectrum acquisition.

**<sup>31</sup>P Solution NMR Experiments.** All spectra were recorded on a Varian Inova Unity 600 (Agilent, Santa Clara, CA) spectrometer operating at a frequency of 246.86 MHz for <sup>31</sup>P and equipped with a 5 mm double-resonance probe. A single-pulse experiment was employed with a  $\pi/2$  pulse of 13.3  $\mu$ s, a recycle delay of 5 s, and an acquisition time of 1 s with broadband proton continuous wave decoupling at a field strength of 5 kHz. A preacquisition delay of 15 min was used before each experiment to ensure sample thermal equilibration. Spectra were acquired at least in triplicate with 32 to 512 scans at 25 °C unless otherwise specified. They were referenced internally using a sealed capillary containing phosphate ions at pH = 11 in D<sub>2</sub>O which was previously referenced with respect to 85% H<sub>3</sub>PO<sub>4</sub> at 3.38 ppm. All spectra were processed using MNova software (Mestrelab Research, Santiago de Compostela, Spain).

**FTIR Experiments.** Infrared spectra were recorded with a Nicolet Magna-560 Fourier transform spectrometer (Thermo Scientific, Madison, WI) equipped with a narrow-band mercury–cadmium–telluride (MCT) detector and a germanium-coated KBr beamsplitter. A volume of 30  $\mu$ L of the 400 mM bicelle sample was placed between CaF<sub>2</sub> Biocell windows (Biotoools Inc., Jupiter, FL) manufactured with a calibrated path length of 50  $\mu$ m. The windows were placed in a homemade heating cell using a Peltier element as a heating/cooling device. To prevent solvent evaporation during the course of long-term measurements, the sealing surface of the cell was lubricated with mineral oil. A total of 128 interferograms were acquired with a resolution of 2 cm<sup>−1</sup> apodized with a Happ-Genzel function in the spectral range of 4000–650 cm<sup>−1</sup> at various temperatures ranging from 5 to 70°. Spectra were corrected for water vapor and CaF<sub>2</sub> contributions by subtraction of a reference spectrum. Data were processed with the software Grams/AI 8.0 (Galactic Industries Corporation, Salem, NH). The spectral regions corresponding to the carbon–hydrogen stretching vibrations were baseline-corrected using a quartic function. The methylene symmetric stretching frequency was obtained from the center of gravity calculated at the top 10% of the band.

**Molecular Dynamics Simulations.** Three sets of MD simulations were performed at 310 K, namely, a self-assembly of DMPC/DHPC at  $q$  of 0.25 (350 ns), the relaxation of an ideal DMPC/DHPC bicelle at  $q$  of 0.25 (450 ns), and the self-assembly of pure DHPC in water (60 ns), aimed at validating the DHPC model. Each simulation box contained 200 lipid molecules (200 DHPC or 160 DHPC + 40 DMPC) in a volume of about 850 nm<sup>3</sup>, yielding a total lipid concentration of 400 mM, and 130 mM NaCl. Each simulation system contained about 80 000 atoms. Lipids were described by the CHARMM36 force field,<sup>43</sup> in our modified version with united-atom acyl chains;<sup>44</sup> the water model was TIP3P. Both the all-atom force field and its united-atom modification are extensively validated against experimental data; the united-atom version enhances the relaxation kinetics of the lipids while reducing computational cost, leading to improved sampling. All simulations were run using the NAMD 2.9 software package<sup>45</sup> on the SGI Altix supercomputer Jade at CINES (Montpellier, France). Self-assembly simulations were started from randomly distributed solutes prepared with the GROMACS tool genbox.<sup>46</sup> The ideal bicelle system was prepared by cutting a disc out of a pre-equilibrated DMPC bilayer, and inserting it in a water environment with randomly placed DHPC molecules. The DMPC bilayer structure was preserved by positional restraints applied to the DMPC headgroups. After 30 ns of simulation, the restraints were lifted to let the overall structure relax.

DMPC/DHPC aggregation was analyzed using a customized version of the *g\_clustsize* tool from GROMACS 4.5.5.<sup>46</sup> Hydrophobic clusters were detected by restricting the analysis to united-atom

particles forming the acyl chains of the lipid and detergent. A cutoff distance of 4.1 Å was chosen in order to include all contact peaks of the interparticle radial distribution function, while minimizing the contribution of short-lived contacts, detected in the form of high-frequency noise in the cluster size dependence as a function of time. Chain order in DMPC was quantified by measuring the distribution of torsional angles between neighboring acyl chains (with centers less than 10 Å away). The direction of each myristoyl chain was computed as the principal axis of inertia with the lowest eigenvalue; the analysis was implemented within the LOOS framework.<sup>47</sup>

## RESULTS AND DISCUSSION

**Exact Composition of Bicelles under Dilution: <sup>31</sup>P NMR.** The long and short-chain phosphatidylcholines constituting the bicelles comprise a single phosphorus atom in their polar headgroup. The high gyromagnetic ratio of the <sup>31</sup>P isotope as well as its 100% natural abundance leads to an easily detectable NMR signal which is dominated by the chemical shift anisotropy (CSA). The resulting spectra are characteristic of the lipid phases present in the sample.<sup>48</sup> However, the CSA is averaged by the fast tumbling of bicelles at low *q* ratios, resulting in an isotropic resonance for each lipid which can be exploited to obtain information on their environment and dynamics.

<sup>31</sup>P NMR spectra of DMPC/DHPC bicelles were recorded for *q* ratios ranging between 0 (pure DHPC) and 2 in water. An example is given in Figure 1 for spectra obtained at *q* = 1 and concentrations decreasing from 400 to 2 mM. For concentrated solutions at a magnetic field of 14.1 T, two resonances can be resolved. The broader upfield signal at ca. −0.50 ppm is

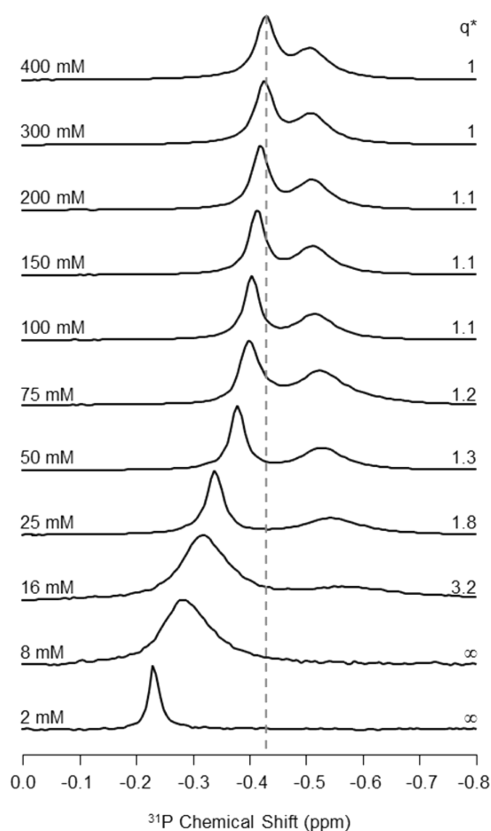


**Figure 1.** Evolution of the <sup>31</sup>P NMR spectrum of bicelles with *q* = 1 as a function of dilution. The calculated effective *q* (*q*\*) is indicated. Data were obtained at 25 °C.

assigned to the long-chain DMPC, whereas the narrow downfield signal is ascribed to DHPC.<sup>2</sup> As the sample is diluted, DMPC's resonance gradually broadens until it completely disappears at 8 mM, while its chemical shift slightly decreases from −0.51 to −0.58 ppm. For concentrations above 25 mM the DMPC/DHPC molar ratio calculated from the integrals of the two lipid resonances on the <sup>31</sup>P NMR spectra is in agreement with the *q* value. DMPC molecules appear to be part of rapidly reorienting aggregates as suggested by the relative resolution of the peak compared to the one obtained with DMPC vesicles. Interestingly, sample turbidity could be observed at higher dilutions (<25 mM) and with *q* ratios ≥0.75 (Figure S1, Supporting Information). This phenomenon is expected if aggregates with characteristic sizes on the order of the visible wavelength are present.<sup>42</sup>

In contrast to the behavior of DMPC's resonance, the narrow DHPC signal remains sharp down to a concentration of 25 mM, then broadens with a full width at half-maximum (fwhm) of 7 to 25 Hz between 25 and 8 mM, to finally sharpen again at 2 mM (fwhm of 5 Hz). In addition, its chemical shift increases with dilution, from −0.43 ppm at 400 mM to −0.23 ppm at 2 mM, a value similar to the <sup>31</sup>P chemical shift of free DHPC molecules in solution (−0.23 ppm) (data not shown). The variation of DHPC <sup>31</sup>P chemical shift value with concentration has been previously explained as resulting from the fast exchange between the bulk solution and the bicelles.<sup>37</sup> As a consequence, the chemical shift value observed on the spectrum ( $\delta_{\text{obs}}$ ) is a weighted average of the chemical shifts of the free ( $\delta_{\text{free}}$ ) and bicelle-bound ( $\delta_{\text{bic}}$ ) DHPC molecules:

$$\delta_{\text{obs}} = \chi_{\text{free}} \delta_{\text{free}} + \chi_{\text{bic}} \delta_{\text{bic}} \quad (1)$$

where  $\chi_i$  corresponds to the molar fractions of DHPC molecules in solution and in the bicelles. Equation 1 can be rearranged to obtain the following expression:

$$\delta_{\text{obs}} = \frac{[\text{DHPC}]_{\text{free}}}{[\text{DHPC}]_{\text{total}}} (\delta_{\text{free}} - \delta_{\text{bic}}) + \delta_{\text{bic}} \quad (2)$$

Therefore, a plot of  $\delta_{\text{obs}}$  as a function of the inverse of the total DHPC concentration ( $1/[\text{DHPC}]_{\text{total}}$ ) should yield a straight line from which  $\delta_{\text{bic}}$  can be extracted as the y-intercept and the concentration of free DHPC can be determined using the slope and a  $\delta_{\text{free}}$  value of −0.23 ppm obtained for a pure DHPC solution at 2 mM. We carried out this systematic analysis for bicelles with *q* of 0.15 to 2 at concentrations ranging between 400 and 25 mM where DHPC molecules are in fast exchange between the bulk solution and fast-tumbling bicelles. The result is presented in Figure S2 in the Supporting Information for *q* = 1 as a representative example. In this case,  $\delta_{\text{bic}}$  is equal to −0.43 ppm, the slope is equal to 1.15, and therefore the concentration of free DHPC is 5.6 mM. For all the *q* values studied in this work, the fast-exchange model appears to be a good approximation with correlation coefficients of the linear fits greater than 0.95. For each *q* value, the concentration of free DHPC which is present in bicelle samples can be referred to as a “critical bicelle concentration” (CBC), in analogy with a critical micelle concentration (CMC), and the average values obtained for triplicates are reported in Figure 3 as a function of all *q* ratios studied.

Figure 2 shows that the extreme case of pure DHPC (*q* = 0) gives an average CMC of 16.5 mM, consistent with the literature value of 16 mM reported for this detergent.<sup>49</sup> As the



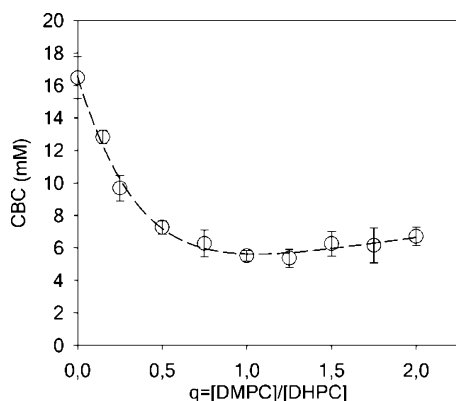


**Figure 2.** Evolution of the critical bicelle concentration (CBC) as a function of  $q$ . Average values ( $n = 3$ ) determined at 25 °C with standard deviation. The dotted line is a guide to the eye. The CMC for ideally mixed bicelles ( $\text{CMC}_{\text{mix}}$ ) is indistinguishable from the zero horizontal axis at the scale of this figure for all  $q$  values. Note that at  $q = 0$ ,  $\text{CBC} = \text{CMC}_{\text{DHPC}}$ .

sample is enriched in DMPC, the CBC gradually decreases to a value of 6.0 mM at  $q = 1$ . This result is in excellent agreement with published CBC values of 4 (at 15 and 37 °C) and 7 mM (at 25 °C) for DMPC/DHPC bicelles at  $q = 0.5^{37,50}$  or CBC values estimated to 7–10 mM (from 28 to 40 °C) for high  $q$  values ( $q = 2.3$ – $3.3$ ).<sup>51</sup> As the system is further enriched in DMPC, the CBC is stable with possibly a slight increase up to a value of 6.7 mM at  $q = 2$ , but this increase is within the experimental error.

Our results were obtained at 25 °C, but they can be generalized to temperatures up to 40 °C. Indeed, it has been shown that the CMC of DHPC micelles is almost constant between 11 and 50 °C.<sup>52</sup> A similar study in bicelles at  $q = 0.5$  also showed no difference in the concentration of free DHPC between 15 and 37 °C.<sup>37</sup> Nevertheless, we verified possible temperature effects on the CBC for  $q = 1$  at 25, 37, and 50 °C and found similar results (data not shown), confirming that the CBC is stable in this temperature range.

To take into account the presence of a non-negligible concentration of free DHPC in the bicelle mixture, which corresponds to the CBC, the effective DMPC/DHPC molar ratio ( $q^*$ ) in the bicellar objects can be calculated, as proposed by Glover et al.:<sup>37</sup>

$$q^* = \frac{[\text{DMPC}]}{[\text{DHPC}] - \text{CBC}} \quad (3)$$

The effect of the dilution on the effective molar ratio  $q^*$  for several theoretical  $q$  ratios (known from the mass of the lipid powders used during sample preparation) is presented in Figure 3 (top). Conversely, and in order to guide the experimentalist, the values of  $q^*$  as a function of  $q$  for different total lipid concentrations are plotted in Figure 3 (bottom). Our results clearly show that attention must be paid when samples are prepared in diluted conditions (i.e.,  $\leq 100$  mM) and especially at high  $q$  ratios ( $q \sim 1.5$ – $2$ ). Indeed under such conditions, the actual DMPC/DHPC molar ratio  $q^*$  in the bicelles strongly deviates from the expected  $q$  ratio. As a result, even a moderate dilution could lead to  $q^* \geq 2.3$ , where the formation of large and slow-tumbling lipid structures that could hinder the use of solution-state NMR methods are observed. For example, for  $q = 1$  at a total lipid concentration of 16 mM, a

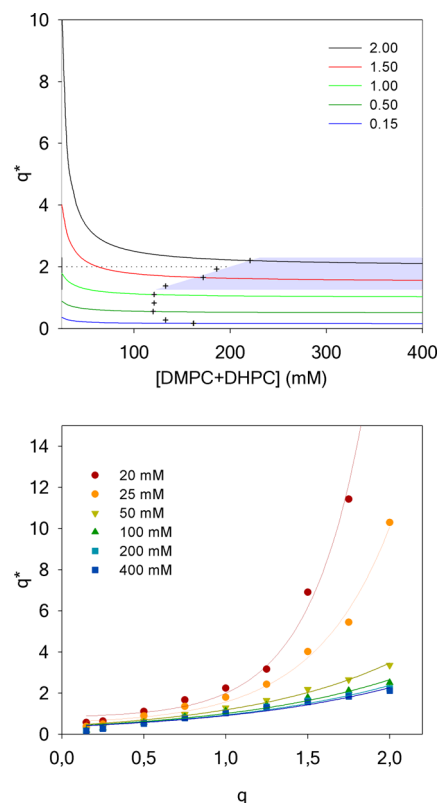


**Figure 3.** Evolution of the effective  $q^*$  for DMPC/DHPC isotropic bicelles as a function of sample dilution for several  $q$  ratios determined at 25 °C (top). The gray zone is the region where bicelles are isotropic, i.e., below  $q^*$  of 2.3 (limit of isotropic motion), above  $q^* = 1$  (lipid segregation between DMPC and DHPC), and  $q^* = q + 10\%$  (crosses). Value of  $q^*$  as a function of  $q$  for different total lipid concentrations (bottom). Solid lines are a guide to the eye.

$q^*$  of 3.2 is found. The  $q^* \leq 2.3$  limit is indicated as a dashed line in Figure 3.

By indicating  $q^*$  on the  $^{31}\text{P}$  NMR spectra in Figure 1, it is possible to better understand the behavior of bicelles under dilution. From 400 to 100 mM, the effective  $q^*$  is very close to 1, the value expected from the sample preparation. With further dilution from 75 to 25 mM,  $q^*$  increases up to 1.8, an effective  $q$  ratio at which isotropic bicelles still prevail. When reaching 16 mM, a  $q^*$  of 3.2 is calculated and corresponds to large bicelles that would orient in the magnetic field if the concentration were higher.<sup>51</sup> Additional dilution of the bicelle samples led to an infinite  $q^*$ , that is, DMPC vesicles are formed. Note that at such low concentrations, the broad spectra which are expected for MLVs could not be detected.

Using the effective  $q^*$  and assuming bicelles are disk-shaped, it is possible to calculate the actual size of the bicelles using the following equation modified from Triba et al.:<sup>12</sup>

$$R = \frac{r_{\perp} q^*}{4\lambda} \left[ \pi + \left( \pi^2 + \frac{32\lambda}{3q^*} \right)^{1/2} \right] \quad (4)$$

where  $R$  is the bicelle disk radius,  $r_{\perp}$  is the length of a DHPC molecule (1.1 nm), and  $\lambda$  is the volume ratio of DHPC over DMPC (0.61).<sup>12</sup> A bicelle with  $q = 1$  for example would have a diameter of  $\sim 65$  Å. The results of the calculation (Table S1, Supporting Information) show an increase in the bicelle diameter for the same sample up to  $\sim 190$  Å when it is diluted

to a total lipid concentration of 16 mM ( $q^* = 3.2$ ). Variation of the concentration of free DHPC molecules at strong dilutions, and its resulting effect on bicelle size, clearly needs to be taken into account when interpreting lateral diffusion data. This is especially the case if geometrical parameters of the bicelles are inferred from diffusion data.<sup>53</sup>

**Lipid Concentration Threshold to Maintain the Desired  $q$  Ratio with Isotropic Bicelles.** In order to ensure that solution NMR experiments are carried out with fast-tumbling bicelles at the desired DMPC/DHPC molar ratio  $q$ , we have determined the total lipid concentration threshold that should be used. To do so, a 10% deviation from the desired  $q$  ratio was considered as acceptable. Replacing  $q^*$  by  $1.1 \times q$  in eq 3 leads to a definition of the minimum lipid concentration threshold:

$$q^* = \frac{[\text{DMPC}]}{[\text{DHPC} - \text{CBC}]} \leq 1.1 \times q \quad (5)$$

which can be rearranged to define a minimal total lipid concentration for a given  $q$  ratio:

$$[\text{DMPC} + \text{DHPC}] = 11 \times \text{CBC} \times (q + 1) \quad (6)$$

The minimum total lipid concentration thresholds to be used at  $q$  ratios ranging from 0.15 to 2 calculated from eq 6 are presented in Table S2 in the Supporting Information and plotted in Figure 3 as crosses.

#### Lipid Miscibility in Bicelles: Comparing CBC and CMC.

The use of bicelles to study the membrane interaction of drugs, peptides, or other molecules, or to determine the structure of membrane-associating peptides is often motivated by the presence of a flat DMPC-rich region in these aggregates. In this section, we verify lipid miscibility as a function of  $q$ . The fact that the CBC value at  $q \geq 1$  ( $\sim 6$  mM) is lower than the CMC of pure DHPC (16 mM) indicates that the DMPC molecules stabilize DHPC molecules into bicellar aggregates.<sup>54</sup> It is interesting to compare the CBC determined from our analysis to the CBC that would be obtained if DMPC and DHPC would form an ideal mixed micelle ( $\text{CMC}_{\text{mix}}$ ) which can be calculated as follows:<sup>54</sup>

$$\frac{1}{\text{CMC}_{\text{mix}}} = \frac{\chi_1}{\text{CMC}_1} + \frac{1 - \chi_1}{\text{CMC}_2} \quad (7)$$

where  $\text{CMC}_i$  is the CMC value of each pure surfactant and  $\chi_1$  is the molar fraction of surfactant 1. With  $\text{CMC}_{\text{DHPC}} = 16$  mM and  $\text{CMC}_{\text{DMPC}} = 6$  mM,<sup>52</sup>  $\text{CMC}_{\text{mix}}$  values between 46 and 9 nM would be expected for  $q$  values between 0.15 and 2, respectively. The plot of  $\text{CMC}_{\text{mix}}$  as a function of  $q$  ratio for an ideal mixed bicelle thus becomes virtually indistinguishable from the horizontal axis in Figure 2. The CBCs determined from our experimental results for the same  $q$  values range between 13 and 5 mM.

The discrepancy between the experimental curve and the ideal mixing curve (Figure 2) shows that the partitioning of both lipids between solution and the aggregate strongly deviate from an ideal mixed micelle, suggesting that the two lipids are at least partially segregated within the bicelle. To verify this hypothesis, FTIR experiments and molecular dynamics simulations were performed.

**$q \geq 1$ : FTIR Spectra Confirm Lipid Segregation in Isotropic Bicelles.** In order to study the degree of miscibility between DMPC and DHPC in bicelles, we measured the thermotropic behavior of these lipids at different  $q$  ratios and

high total lipid concentration (400 mM) by FTIR spectroscopy. This was done by using protonated DHPC and DMPC with perdeuterated acyl chains ( $\text{DMPC-}d_{54}$ ), and plotting the  $\text{CD}_2$  symmetric stretching frequency ( $\sim 2090 \text{ cm}^{-1}$ ) as a function of temperature. The methylene stretching vibrations in lipid acyl chains are sensitive to changes in the trans/gauche conformer ratio and allow probing the transition between an ordered gel to more disordered liquid crystalline phase.<sup>55</sup> In the case of an ideal homogeneous mixture, the melting temperature ( $T_m$ ) can be calculated considering the respective  $T_m$  and mole fractions of the lipids:<sup>49</sup>

$$T_m^{\text{bic}} = \chi_{\text{DHPC}} T_m^{\text{DHPC}} + \chi_{\text{DMPC}} T_m^{\text{DMPC}} \quad (8)$$

where the  $T_m$  of DHPC and DMPC- $d_{54}$  are  $-46^{\circ}\text{C}$ <sup>56</sup> and  $21^{\circ}\text{C}$  (experimental value), respectively. The thermotropic behavior of DMPC- $d_{54}$  is shown in Figure 4 (top) as well as the variation

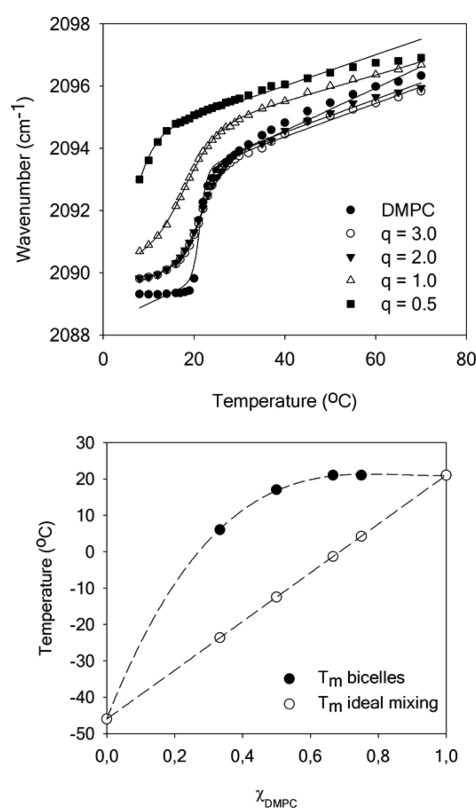


**Figure 4.** Temperature dependence of the wavenumber of the  $\text{CD}_2$  symmetric stretching vibration in bicelles with varying  $q$  ratios (top). Determined melting temperatures ( $T_m$ ) for bicelles and calculated for an ideal mixture (bottom) as a function of DMPC molar fraction. Dotted lines are a guide to the eye.

of the melting temperature with DMPC- $d_{54}$  molar fraction compared to the variation expected for an ideal mixed micelle (bottom). The experimental and ideal melting temperatures are reported in Table S3 in the Supporting Information. The  $T_m$  of  $21^{\circ}\text{C}$  obtained from the infrared spectroscopy analysis is constant when  $q$  is superior to 1 and corresponds to that of pure DMPC- $d_{54}$ . Moreover, the values of the  $\text{CD}_2$  symmetric stretching frequencies are almost superimposable in the fluid phase, indicating that the acyl chain ordering is not affected by the presence of DHPC. These results suggest that DMPC is largely segregated in the planar section of bicelles when  $q > 1$ . As the  $q$  ratio is decreased, the discrepancy between the

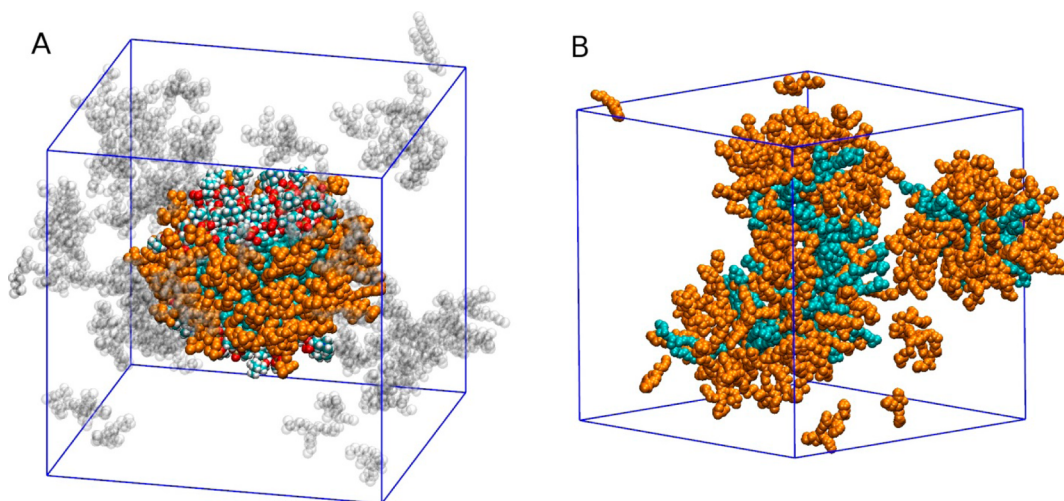


**Figure 5.** Simulation of a bicelle at  $q^* = 0.25$ . (A) Ideal bicellar assembly obtained by restraining DMPC lipid positions. Cyan, DMPC (headgroup atoms colored by element); orange, bicellar DHPC; transparent, micellar and free DHPC molecules. The simulation periodic box is outlined in blue. (B) Same system after 300 ns of MD relaxation at 310 K. All DHPC molecules colored orange.

experimental  $T_m$  of DMPC- $d_{54}$  in bicelles and the calculated  $T_m$  of DMPC- $d_{54}$  in an ideal mixed micelle diminishes, showing progressive mixing of DMPC and DHPC molecules, even though bicelles retain some level of bilayer content and anisotropy, as observed by Glover and colleagues.<sup>37</sup> The  $CD_2$  symmetric stretching frequencies augment in both the gel and fluid phases due to an increased disordering of DMPC acyl chains, probably caused by the proximity of mobile DHPC molecules. Interestingly, Andersson and Mäler<sup>57</sup> have shown that the lipids' local mobility at  $q = 0.25$  and  $0.5$  is more affected by the nature of the surfactant than the overall size of the bicelle. This influence is consistent with the mixing at these low  $q$  ratios found in our work. It would be of interest to study bicelles at lower  $q$  ratios; however, the melting temperatures drop below the freezing point of water and hinder such monitoring. Therefore, to study the mixing behavior of DMPC and DHPC in such conditions, molecular dynamics simulations were performed at a  $q$  of  $0.25$ .

**$q \leq 0.5$ : Molecular Dynamics Simulations Show Lipid Mixing in Very Small Bicelles.** An ideal bicelle assembly at  $q^* = 0.25$ , completely segregated and disc shaped, was obtained by letting DHPC molecules self-assemble around a bilayer patch of DMPC molecules with restrained positions (Figure 5A). The same system after 300 ns of unrestrained MD relaxation at 310 K is shown in Figure 5B. Our simulations give free DHPC concentrations of  $34 \pm 8$  mM (pure DHPC/water) and  $21 \pm 6$  mM (DMPC/DHPC self-assembly). This is higher than the experimental CMC/CBC in the same conditions, but within a factor of 2, indicating that the free energy of aggregation of the model is underestimated by less than the thermal energy  $RT$ . The atomistic model thus possesses chemical accuracy, unlike coarse-grained models that give access to much larger space and time scales, at the expense of capturing the specifics of any particular chemical system.<sup>58</sup>

The self-assembly simulation started with randomly distributed DMPC and DHPC molecules in solution. It showed a rapid aggregation on the nanosecond time scale, followed by slower rearrangement and fluctuations of the aggregates that, like the one in Figure 5B, were not disc-shaped and did not exhibit bilayer-like regions or notable DMPC clusters. This result could also be observed for thermodynamically stable

disk-like bicelles if their formation required slow ordering and segregation of the components that could not occur within the 350 ns self-assembly simulation for kinetic reasons. To test this hypothesis, we also performed a separate simulation starting from an "ideal" bicelle in which DMPC and DHPC molecules were completely segregated. In the first 30 ns, DMPC molecules were artificially restrained to preserve the bilayer arrangement, and DHPC molecules spontaneously assembled on the edges, thus forming a canonical disc-shaped bicelle as shown in Figure 5A. After 30 ns, DMPC restraints were lifted and a rapid mixing ensued, leading to mixed micelles (Figure 5B) comparable to those observed under self-assembly conditions. In general, atomistic simulations of such systems may suffer from metastability due to time scale limitations. Here, we crucially obtained the same final structure starting from different states, showing that the mixed micelle is the most kinetically accessible aggregate from a random dispersion, but also that a perfectly segregated bicelle is unstable. Together, these simulations clearly predict a thermodynamic tendency of DHPC and DMPC molecules to mix and form small aggregates devoid of a bilayer-like region, at very low  $q$  ratios.

The ideal segregated bicelle prior to relaxation exhibits collective acyl chain order typical of a bilayer rearrangement, with a distribution of torsion angles between neighboring chains peaked around 0, as shown in Figure 6A. In sharp contrast, the DMPC/DHPC aggregates formed after relaxation show a much broader distribution of angles between the neighboring myristoyl chains. Correspondingly, the black lines in Figure 6B indicate a strong ordering in the ideal segregated bicelle system, where the DMPC bilayer region is indeed enriched in DMPC. In contrast, the data obtained (in red) from the aggregates formed after bicelle relaxation show very weak enrichment, denoting significant yet imperfect lipid mixing. Thus, for bicelles with  $q < 1$  where infrared studies suggest some lipid segregation, our simulations predict a nonideal behavior intermediate between that of pure DMPC and an ideal homogeneous mixture of DMPC and DHPC.

Altogether, our results suggest that for studies where a bilayer-like region is required, bicelles with a  $q > 1$  should be utilized. Note that in such conditions the correlation times of bicelles will be long and consequently resonances will be



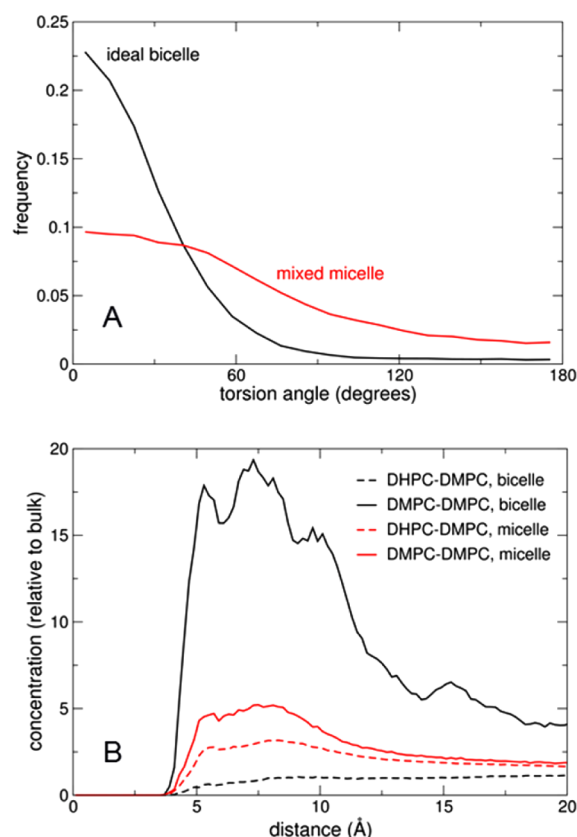


**Figure 6.** Lipid mixing and ordering in the simulated low- $q^*$  mixture. (A) Distribution of torsion angles between neighboring myristoyl chains in DMPC, in the ideal bicelle model (black) and after unrestrained relaxation (red). (B) Radial distribution functions of glycerol C2 atoms between DMPC molecules (solid lines) and between DHPC and DMPC (dashed lines), in the ideal bicelle (black) and unrestrained mixed micelle (red).

broadened thus potentially hindering the study of integral membrane proteins. The  $q$  ratio boundaries, where DMPC and DHPC are expected to be segregated while still forming aggregates which reorient rapidly in the magnetic field, and the lower limit of the total lipid concentration where expected and actual  $q$  ratios vary by less than 10%, define the ideal work region which is highlighted in gray in Figure 3.

## CONCLUSION

Low  $q$  DMPC/DHPC bicelles were studied by  $^{31}\text{P}$  NMR, FTIR spectroscopy, and molecular dynamics. The critical bicellar concentration (CBC) was introduced as an important parameter which allows determining the exact long-to-short chain lipid ratio in the system and the diameter of the bicelle. This knowledge is necessary to improve sample control for experiments requiring small membrane objects such as solution NMR, or diluted conditions such as CD or DLS. Finally, the word “bicelle” appears to be a misnomer for  $q$  ratios below 1 where lipid complexes would be more accurately described as mixed micelles.

## ASSOCIATED CONTENT

### Supporting Information

Visual aspect of the bicelle samples at different lipid concentrations and molar ratios. Bicelle radius calculated for  $q = 1$  from the effective  $q$  value ( $q^*$ ). Observed  $^{31}\text{P}$  chemical

shift of DHPC as a function of the inverse of DHPC concentration in DMPC/DHPC mixtures with  $q = 1$ . Minimal total phospholipid concentration recommended to conserve the desired bicelle molar ratio  $q$ . Comparison of the experimental melting temperature of DMPC- $d_{54}$  in bicelles with values expected in ideal mixed micelles at different  $q$  ratios. This material is available free of charge via the Internet at <http://pubs.acs.org>.

## AUTHOR INFORMATION

### Corresponding Author

\*E-mail: [marcotte.isabelle@uqam.ca](mailto:marcotte.isabelle@uqam.ca).

### Notes

The authors declare no competing financial interest.

## ACKNOWLEDGMENTS

This work was supported by the Natural Sciences and Engineering Research Council (NSERC) of Canada. P.T.F.W. would like to acknowledge financial support from the Wellcome Trust (Grant No. 090658/Z/09/Z). M.B. wishes to thank the *Université du Québec à Montréal*, the Training Program in Bionanomachines (NSERC), the Canadian Institutes of Health Research Strategic Training Initiative in Chemical Biology, and the *Centre Québécois sur les Matériaux Fonctionnels* (CQMF) for the award of scholarships. This work was granted access to the HPC resources of CINES (Montpellier, France) under the allocation x2013077058 made by GENCI (Grand Équipement National de Calcul Intensif). Dr. A. Grossfield is gratefully acknowledged for providing custom simulation analysis tools. I.M. is a member of the CQMF and the Groupe de Recherche Axé sur la Structure des Protéines (GRASP).

## REFERENCES

- (1) Sanders, C. R.; Prestegard, J. H. Magnetically Orientable Phospholipid Bilayers Containing Small Amounts of a Bile Salt Analogue, CHAPSO. *Biophys. J.* **1990**, *58*, 447–460.
- (2) Sanders, C. R.; Schwonek, J. P. Characterization of Magnetically Orientable Bilayers in Mixtures of Dihexanoylphosphatidylcholine and Dimyristoylphosphatidylcholine by Solid-State NMR. *Biochemistry* **1992**, *31*, 8898–8905.
- (3) Dürr, U. H. N.; Soong, R.; Ramamoorthy, A. When Detergent Meets Bilayer: Birth and Coming of Age of Lipid Bicelles. *Prog. Nucl. Magn. Reson. Spectrosc.* **2013**, *69*, 1–22.
- (4) Marcotte, I.; Auger, M. Bicelles as Model Membranes for Solid- and Solution-State NMR Studies of Membrane Peptides and Proteins. *Concepts Magn. Reson., Part A* **2005**, *24A*, 17–37.
- (5) Warschawski, D. E.; Arnold, A. A.; Beaugrand, M.; Gravel, A.; Chartrand, É.; Marcotte, I. Choosing Membrane Mimetics for NMR Structural Studies of Transmembrane Proteins. *Biochim. Biophys. Acta* **2011**, *1808*, 1957–1974.
- (6) Cross, T. A.; Sharma, M.; Yi, M.; Zhou, H.-X. Influence of Solubilizing Environments on Membrane Protein Structures. *Trends Biochem. Sci.* **2011**, *36*, 117–125.
- (7) Chou, J. J.; Kaufman, J. D.; Stahl, S. J.; Wingfield, P. T.; Bax, A. Micelle-Induced Curvature in a Water-Insoluble HIV-1 Env Peptide Revealed by NMR Dipolar Coupling Measurement in Stretched Polyacrylamide Gel. *J. Am. Chem. Soc.* **2002**, *124*, 2450–2451.
- (8) Thiagarajan, P.; Tiede, D. M. Detergent Micelle Structure and Micelle-Micelle Interactions Determined by Small-Angle Neutron Scattering under Solution Conditions Used for Membrane Protein Crystallization. *J. Phys. Chem.* **1994**, *98*, 10343–10351.
- (9) Barbosa-Barros, L.; Rodríguez, G.; Cócera, M.; Rubio, L.; López-Iglesias, C.; De La Maza, A.; López, O. Structural Versatility of Bicellar

Systems and Their Possibilities as Colloidal Carriers. *Pharmaceutics* **2011**, *3*, 636–664.

(10) Diller, A.; Loudet, C.; Aussenac, F.; Raffard, G.; Fournier, S.; Laguerre, M.; Grélaud, A.; Opella, S. J.; Marassi, F. M.; Dufourc, E. J. Bicelles: A Natural “Molecular Goniometer” for Structural, Dynamical and Topological Studies of Molecules in Membranes. *Biochimie* **2009**, *91*, 744–751.

(11) Ram, P.; Prcestegard, J. H. Magnetic Field Induced Ordering of Bile Salt/phospholipid Micelles: New Media for NMR Investigations. *Biochim. Biophys. Acta* **1988**, *940*, 289–294.

(12) Triba, M. N.; Warschawski, D. E.; Devaux, P. F. Reinvestigation by Phosphorus NMR of Lipid Distribution in Bicelles. *Biophys. J.* **2005**, *88*, 1887–1901.

(13) Sanders, C. R.; Prosser, R. S. Bicelles: A Model Membrane System for All Seasons? *Structure* **1998**, *6*, 1227–1234.

(14) Naito, A. Structure Elucidation of Membrane-Associated Peptides and Proteins in Oriented Bilayers by Solid-State NMR Spectroscopy. *Solid State Nucl. Magn. Reson.* **2009**, *36*, 67–76.

(15) Faham, S.; Ujwal, R.; Abramson, J.; Bowie, J. U. Practical Aspects of Membrane Proteins Crystallization in Bicelles. *Curr. Top. Membr.* **2009**, *63*, 109–125.

(16) Seddon, A. M.; Curnow, P.; Booth, P. J. Membrane Proteins, Lipids and Detergents: Not Just a Soap Opera. *Biochim. Biophys. Acta* **2004**, *1666*, 105–117.

(17) Macdonald, P. M.; Saleem, Q.; Lai, A.; Morales, H. H. NMR Methods for Measuring Lateral Diffusion in Membranes. *Chem. Phys. Lipids* **2013**, *166*, 31–44.

(18) Yamamoto, K.; Percy, P.; Ramamoorthy, A. Bicelles Exhibiting Magnetic Alignment for a Broader Range of Temperatures: A Solid-State NMR Study. *Langmuir* **2014**, *30*, 1622–1629.

(19) Katsaras, J. Alignable Biomimetic Membranes. *Phys. B* **1998**, *241–243*, 1178–1180.

(20) Sanders, C. R.; Hare, B. J.; Howard, K. P.; Prestegard, J. H. Magnetically-Oriented Phospholipid Micelles as a Tool for the Study of Membrane-Associated Molecules. *Prog. NMR Spectrosc.* **1994**, *26*, 421–444.

(21) Sanders, C. R.; Landis, G. C. Facile Acquisition and Assignment of Oriented Sample NMR Spectra for Bilayer Surface-Associated Proteins. *J. Am. Chem. Soc.* **1994**, *116*, 6470–6471.

(22) Ottiger, M.; Bax, A. Characterization of Magnetically Oriented Phospholipid Micelles for Measurement of Dipolar Couplings in Macromolecules. *J. Biomol. NMR* **1998**, *12*, 361–372.

(23) Yamamoto, K.; Soong, R.; Ramamoorthy, A. Comprehensive Analysis of Lipid Dynamics Variation with Lipid Composition and Hydration of Bicelles Using Nuclear Magnetic Resonance (NMR) Spectroscopy. *Langmuir* **2009**, *25*, 7010–7018.

(24) Luchette, P. A.; Vetman, T. N.; Prosser, R. S.; Hancock, R. E. W.; Nieh, M.-P.; Glinka, C. J.; Krueger, S.; Katsaras, J. Morphology of Fast-Tumbling Bicelles: A Small Angle Neutron Scattering and NMR Study. *Biochim. Biophys. Acta* **2001**, *1513*, 83–94.

(25) Vold, R. R.; Prosser, R. S.; Deese, A. J. Isotropic Solutions of Phospholipid Bicelles: A New Membrane Mimetic for High-Resolution NMR Studies of Polypeptides. *J. Biomol. NMR* **1997**, *9*, 329–335.

(26) Marcotte, I.; Separovic, F.; Auger, M.; Gagné, S. M. A Multidimensional  $^1\text{H}$  NMR Investigation of the Conformation of Methionine-Enkephalin in Fast-Tumbling Bicelles. *Biophys. J.* **2004**, *86*, 1587–1600.

(27) Andersson, A.; Mäler, L. NMR Solution Structure and Dynamics of Motilin in Isotropic Phospholipid Bicellar Solution. *J. Biomol. NMR* **2002**, *24*, 103–112.

(28) Haney, E. F.; Hunter, H. N.; Matsuzaki, K.; Vogel, H. J. Solution NMR Studies of Amphibian Antimicrobial Peptides: Linking Structure to Function? *Biochim. Biophys. Acta* **2009**, *1788*, 1639–1655.

(29) Gravel, A. E.; Arnold, A. A.; Dufourc, E. J.; Marcotte, I. An NMR Investigation of the Structure, Function and Role of the hERG Channel Selectivity Filter in the Long QT Syndrome. *Biochim. Biophys. Acta* **2013**, *1828*, 1494–1502.

(30) Chartrand, E.; Arnold, A. A.; Gravel, A.; Jenna, S.; Marcotte, I. Potential Role of the Membrane in hERG Channel Functioning and Drug-Induced Long QT Syndrome. *Biochim. Biophys. Acta* **2010**, *1798*, 1651–1662.

(31) Andersson, A.; Almqvist, J.; Hagn, F.; Mäler, L. Diffusion and Dynamics of Penetratin in Different Membrane Mimicking Media. *Biochim. Biophys. Acta* **2004**, *1661*, 18–25.

(32) Son, W. S.; Park, S. H.; Nothnagel, H. J.; Lu, G. J.; Wang, Y.; Zhang, H.; Cook, G. A.; Howell, S. C.; Opella, S. J. “Q-Titration” of Long-Chain and Short-Chain Lipids Differentiates between Structured and Mobile Residues of Membrane Proteins Studied in Bicelles by Solution NMR Spectroscopy. *J. Magn. Reson.* **2012**, *214*, 111–118.

(33) Bocharov, E. V.; Mayzel, M. L.; Volynsky, P. E.; Goncharuk, M. V.; Ermolyuk, Y. S.; Schulga, A. A.; Artemenko, E. O.; Efremov, R. G.; Arseniev, A. S. Spatial Structure and pH-Dependent Conformational Diversity of Dimeric Transmembrane Domain of the Receptor Tyrosine Kinase EphA1. *J. Biol. Chem.* **2008**, *283*, 29385–29395.

(34) Mineev, K. S.; Bocharov, E. V.; Volynsky, P. E.; Goncharuk, M. V.; Tkach, E. N.; Ermolyuk, Y. S.; Schulga, A. A.; Chupin, V. V.; Maslennikov, I. V.; Efremov, R. G.; Arseniev, A. S. Dimeric Structure of the Transmembrane Domain of Glycophorin A in Lipidic and Detergent Environments. *Acta Naturae* **2011**, *3*, 90–98.

(35) Surya, W.; Li, Y.; Millet, O.; Diercks, T.; Torres, J. Transmembrane and Juxtamembrane Structure of  $\alpha\text{L}$  Integrin in Bicelles. *PLoS One* **2013**, *8*, e74281.

(36) Biverstahl, H.; Lind, J.; Bodor, A.; Mäler, L. Biophysical Studies of the Membrane Location of the Voltage-Gated Sensors in the HsapBK and KvAP K(+) Channels. *Biochim. Biophys. Acta* **2009**, *1788*, 1976–1986.

(37) Glover, K. J.; Whiles, J. A.; Wu, G.; Yu, N.-J.; Deems, R.; Struppe, J. O.; Stark, R. E.; Komives, E. A.; Vold, R. R. Structural Evaluation of Phospholipid Bicelles for Solution-State Studies of Membrane-Associated Biomolecules. *Biophys. J.* **2001**, *81*, 2163–2171.

(38) Andersson, A.; Mäler, L. Magnetic Resonance Investigations of Lipid Motion in Isotropic Bicelles. *Langmuir* **2005**, *21*, 7702–7709.

(39) Le Maire, M.; Champeil, P.; Moller, J. V. Interaction of Membrane Proteins and Lipids with Solubilizing Detergents. *Biochim. Biophys. Acta* **2000**, *1508*, 86–111.

(40) Kang, C.; Li, Q. Solution NMR Study of Integral Membrane Proteins. *Curr. Opin. Chem. Biol.* **2011**, *15*, 560–569.

(41) van Dam, L.; Karlsson, G.; Edwards, K. Direct Observation and Characterization of DMPC/DHPC Aggregates under Conditions Relevant for Biological Solution NMR. *Biochim. Biophys. Acta* **2004**, *1664*, 241–256.

(42) Lu, Z.; Van Horn, W. D.; Chen, J.; Mathew, S.; Zent, R.; Sanders, C. R. Bicelles at Low Concentrations. *Mol. Pharmaceutics* **2012**, *9*, 752–761.

(43) Klauda, J. B.; Venable, R. M.; Freites, J. A.; O'Connor, J. W.; Tobias, D. J.; Mondragon-Ramirez, C.; Vorobyov, I.; MacKerell, A. D., Jr.; Pastor, R. W. Update of the CHARMM All-Atom Additive Force Field for Lipids: Validation on Six Lipid Types. *J. Phys. Chem. B* **2010**, *114*, 7830–7843.

(44) Hénin, J.; Shinoda, W.; Klein, M. L. United-Atom Acyl Chains for CHARMM Phospholipids. *J. Phys. Chem. B* **2008**, *112*, 7008–7015.

(45) Phillips, J. C.; Braun, R.; Wang, W.; Gumbart, J.; Tajkhorshid, E.; Villa, E.; Chipot, C.; Skeel, R. D.; Kalé, L.; Schulten, K. Scalable Molecular Dynamics with NAMD. *J. Comput. Chem.* **2005**, *26*, 1781–1802.

(46) Pronk, S.; Páll, S.; Schulz, R.; Larsson, P.; Bjelkmar, P.; Apostolov, R.; Shirts, M. R.; Smith, J. C.; Kasson, P. M.; van der Spoel, D.; Hess, B.; Lindahl, E. GROMACS 4.5: A High-Throughput and Highly Parallel Open Source Molecular Simulation Toolkit. *Bioinformatics* **2013**, *29*, 845–854.

(47) Romo, T. D.; Grossfield, A. LOOS: An Extensible Platform for the Structural Analysis of Simulations. *31st Annu. Int. Conf. IEEE EMBS* **2009**, 2332–2335.

(48) Seelig, J.  $^31\text{P}$  Nuclear Magnetic Resonance and the Head Group Structure of Phospholipids in Membranes. *Biochim. Biophys. Acta* **1978**, *515*, 105–140.



- (49) Marsh, D. *Handbook of Lipid Bilayers*; second ed.; CRC Press, Taylor & Francis Group: Boca Raton, FL, 2013; p 307.
- (50) Ramirez, B. E.; Voloshin, O. N.; Camerini-Otero, R. D.; Bax, A. D. Solution Structure of DinI Provides Insight into Its Mode of RecA Inactivation. *Protein Sci.* **2000**, *9*, 2161–2169.
- (51) Struppe, J.; Vold, R. R. Dilute Bicellar Solutions for Structural NMR Work. *J. Magn. Reson.* **1998**, *135*, 541–546.
- (52) Marsh, D. *Handbook of Lipid Bilayers*, second ed.; CRC Press, Taylor & Francis Group: Boca Raton, FL, 2013; p 816.
- (53) Andersson, A.; Mäler, L. Size and Shape of Fast-Tumbling Bicelles as Determined by Translational Diffusion. *Langmuir* **2006**, *22*, 2447–2449.
- (54) Holland, P. M.; Rubingh, D. N. Nonideal Multicomponent Mixed Micelle Model. *J. Phys. Chem.* **1983**, *87*, 1984–1990.
- (55) Mendelsohn, R.; Mantsch, H. H. Fourier Transform Infrared Studies of Lipid-Protein Interaction. In *Progress in Protein-Lipid Interactions*; Elsevier: Amsterdam, 1986; pp 103–146.
- (56) Sakuma, Y.; Taniguchi, T.; Imai, M. Pore Formation in a Binary Giant Vesicle Induced by Cone-Shaped Lipids. *Biophys. J.* **2010**, *99*, 472–479.
- (57) Andersson, A.; Mäler, L. Magnetic Resonance Investigations of Lipid Motion in Isotropic Bicelles. *Langmuir* **2005**, *21*, 7702–7709.
- (58) Vácha, R.; Frenkel, D. Stability of Bicelles: A Simulation Study. *Langmuir* **2014**, *30*, 4229–4235.

#### ■ NOTE ADDED IN PROOF

While the proofs of this article were being prepared, a publication addressing similar issues by other techniques was published by Ye et al. (*Langmuir*, DOI: 10.1021/la500231z). Overall their conclusions are in agreement with ours, although our molecular dynamics simulations point against the disc shape of mixed DMPC/DHPC micelles at low  $q$ . It should be noted that we define the critical bicelle concentration (CBC) as the free concentration of DHPC in solution at which DMPC/DHPC aggregates are formed, in exact analogy to the critical micelle concentration (CMC). Ye et al. describe the CBC as the total lipid concentration at which bilayered bicelles are formed.